Analysis of Backgrounds for a Radon-Emanation System

S.I. Bendigo,[a] N.I. Chott, R.W. Schnee, D.R. Tronstad, and K. Weber

South Dakota School of Mines & Technology, Department of Physics, Rapid City, SD 57701-3901 USA

[a] *Corresponding author: sethbendigo@outlook.com*

Abstract. Expected backgrounds for electrostatic PIN-diode radon-emanation systems consist of three basic terms: a grow-in term, due to radon emanating from the detection chamber itself; a decaying term, due to radon that is transferred into the chamber along with radon from the sample; and a term constant in time due to environmental backgrounds such as cosmic rays. The first two backgrounds should produce energies corresponding to the radon-daughter peaks, while the third is expected to produce a continuous energy spectrum. To determine what is the dominant background for the South Dakota Mines emanation system, many background runs were co-added. Results indicate that environmental backgrounds are small, producing < 0.28 counts/day at 95% confidence in the ^{214}Po energy region of interest (ROI). The grow-in and decay terms are 2.01 ± 0.39 counts/day and 0.95 ± 0.15 counts/day respectively in the same ROI (for the best-fit value for environmental backgrounds). The decay term is larger than expected, so a cold radon trap is now being used to attempt to reduce it.

INTRODUCTION

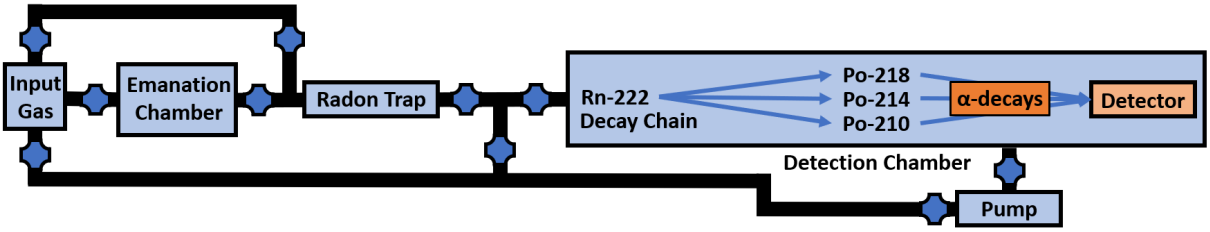

FIGURE 1. A simplified diagram of the radon emanation system at South Dakota Mines. After samples are isolated in the emanation chamber for one to two weeks, the input gas is used to move the radon from the emanation chamber to the radon trap. The trapped radon is then moved to the detection chamber where ^{222}Rn decays into ^{218}Po and its subsequent progeny, whose alpha decays may be detected.

The radon emanation system at South Dakota Mines [1, 2] aims to measure the rate of radon emanating out of samples. Fig. 1 shows a simplified diagram of the system. Samples are isolated in the emanation chamber at low pressure for one to two weeks to allow the radon concentration to grow nearly into equilibrium ($t_{1/2} \approx 3.8$ days) [3, 4]. Liquid nitrogen (LN) boil-off gas is used to flush the gas in the emanation chamber through a cold trap designed to freeze out radon. After the trap is warmed, additional LN boil-off gas flushes the radon into the detection chamber. Inside the detection chamber, ^{222}Rn decays into ^{218}Po, which is positively charged 88% of the time [5]. An electrostatic field moves ^{218}Po^{+} to an α detector where its decay and subsequent α-decays in the chain can be detected. Events in the ^{214}Po (7.7-MeV α) [3, 4] and ^{218}Po (6-MeV α) energy regions of interest (ROIs) are used to find the best-fit estimates of the emanated ^{222}Rn sample rate and the background rate.

A limited number of "blank" runs, which repeat the full emanation and transfer procedure performed with an empty emanation chamber, have been performed to estimate the radon backgrounds associated with the full process of measuring a sample. Results indicate backgrounds of 0.20 ± 0.04 mBq [1, 2]. Additionally, "background" runs, where the chamber is flushed and then filled with boil-off LN gas directly, are performed immediately before and after each sample measurement to check that no significant change in backgrounds has occurred. These background runs give rates about the same as the blank rates, corresponding to about 2 counts/day. For each sample run, the average background rate from the immediate pre-sample and post-sample runs is effectively subtracted from the sample run as part of determining the sample's emanation rate. The statistical uncertainty of this effective subtraction is quite large and so results in conservative uncertainties on sample results while correcting for possible changes in backgrounds.

This work attempts to understand the backgrounds of the system in order to give insight on how to reduce them. There are insufficient statistics to determine the time dependence of an individual background run, but co-adding many background runs provides enough data to analyze the time dependence of the background data.

BACKGROUND MODEL

Before taking data, the detection chamber is flushed of any contents and then filled with LN boil-off gas until the pressure reaches ∼100 Torr. The LN boil-off may carry some amount of radon that does not originate from the sample. The LN boil-off has an expected radon concentration of about 0.5 mBq/m^3 [6], which, in the 1.7-L emanation chamber at 100 Torr, corresponds to 10^{-4} mBq and is therefore negligible. It is not expected that radon daughters are transferred with the gas, in part based on measurements of a ^{220}Rn source that placed stringent limits on the fraction of ^{212}Pb transferred [7]. Some radon may back-diffuse out of plastics in the detection chamber, but this is expected to be negligible except when very high concentrations of radon have just been measured [2]. The decay of the radon transferred into the detection chamber can be modeled as a function of time t by

$$R_{\text{decay}}(t) = D_0 e^{-\lambda t},$$

where the ^{222}Rn decay constant $\lambda \approx 0.00756$ decays/hour [3, 4], and $D_0 = \lambda N_0$ is the initial ^{222}Rn decay rate when N_0 radon atoms are transferred to the detection chamber.

After flushing, ^{226}Ra ($t_{1/2} \sim 1602$ years) in the materials of the detection chamber produce an essentially constant rate E of radon emanation into the chamber's gas, producing a grow-in rate of ^{222}Rn decays:

$$R_{\text{grow}}(t) = E\left(1 - e^{-\lambda t}\right).$$

The combination of R_{grow}, R_{decay}, and a constant term C (accounting for environmental backgrounds interacting in the detector) represents the full background model,

$$R_{\text{bckg}} = R_{\text{grow}} + R_{\text{decay}} + C = E\left(1 - e^{-\lambda t}\right) + D_0 e^{-\lambda t} + C. \tag{1}$$

However, D_0, E, and C are degenerate, so Equation 1 can be re-arranged to

$$R_{\text{fit}} = (E - D_0)\left(1 - e^{-\lambda t}\right) + (C + D_0) = A\left(1 - e^{-\lambda t}\right) + B. \tag{2}$$

This 'grow-in and constant' rearrangement is chosen so that the two parameters to fit (here A and B) are both positive when fit to the data.

ANALYSIS

As the detector records data, its gain can decrease. Past measurements with high rates of ^{218}Po, ^{214}Po, and ^{210}Po indicate that it is only the detector's gain that changes (decreasing from its standard value). The gain as a function of time is determined from the data itself, using the relatively high rate of ^{210}Po decays at 5.3 MeV built up from seven previous years of exposure to Rn measurements (see Fig. 2). Since ^{210}Po's grand-parent ^{210}Pb has $t_{1/2} \sim 22$ years, the rate of ^{210}Po decays is roughly constant with time. For every one-hour time interval (hereafter referred to as a "time bin") in a background run, the channel containing the ^{210}Po peak is determined, the amount of gain needed to shift the peak to 5.3 MeV is calculated, and the gain shift is applied to every channel in that time bin. Aliasing produced by the conversion from channel to energy is corrected.

Some time bins in this data set were dominated by noise that reached energies as high as 8–10 MeV, far beyond the typical noise floor at ≈2.5 MeV (see Fig. 2). Noisy time bins were removed from the background runs. 63 background runs were analyzed. 55 runs required gain correction, 22 runs needed removal of noisy time bins, and 4 runs were removed entirely based on their poor energy resolution (measured using Gaussian curve-fits to the ^{210}Po ROI data of each run), resulting in 59 accepted background runs. These 59 runs were added together by their time bins relative to the start of data-taking for each background run. The result can be seen in the left panel of Fig. 2. Background runs ranged from 21 to 368 time bins in length, with most shorter than 200 time bins. This analysis was cut off at 312 time bins (13 days) due to the lack of statistics at later times. A total of 5990 hours of background runs were included.

An upper bound on C can be estimated from the energy spectrum in the right panel of Fig. 2 under the assumption that time-independent background sources (such as cosmic muons) are monotonically decreasing as a function of energy. A constant plus two Gaussian curves are fit to the data in the ^{216}Po and ^{214}Po ROIs. Although PIN diodes can inherently provide resolutions good enough to reveal the non-Gaussian nature of the alpha peaks, the gain variation

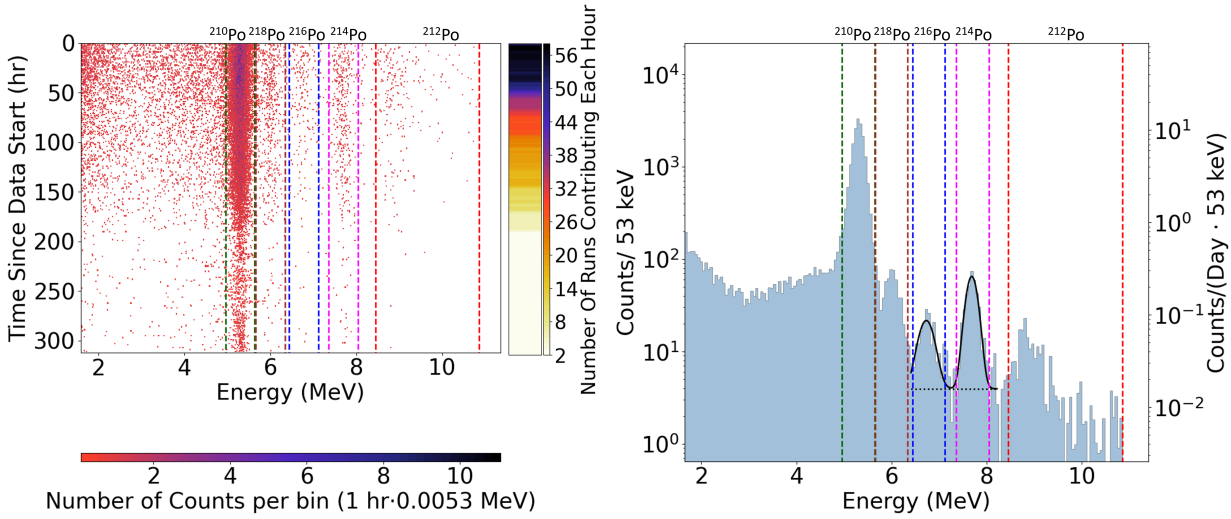

FIGURE 2. Left: 2D Histogram of counts as function of energy and time since run start co-added over all background runs, with 1-hour time bins and 5.3-keV energy bins. ROIs are shown (dashed vertical lines) for ^{210}Po (centered at 5.3 MeV), ^{218}Po (centered at 6.0 MeV), ^{216}Po (centered at 6.78 MeV), ^{214}Po (centered at 7.7 MeV), and ^{212}Po (8.54 MeV–10.85 MeV). The number of runs that contribute data each hour, ranging from 58 for most of the first 20 hours down to 2 for the later hours, is represented by the color plot to the right of the 2D histogram. The decrease in the density of counts, especially visible after 200 hours, is due to fewer runs contributing data at later times. The high density of counts below 5 MeV is due to some runs having more noise at those energies. **Right:** Semi-logarithmic plot of total counts per 53 keV as a function of energy. ROIs are the same as the left plot. Notice the overlap of ^{210}Po events into the ^{218}Po ROI. Counts for ^{212}Po extend to higher energies because of beta decays of ^{212}Bi coincident in the detector with ^{212}Po alpha decays. The sum of two Gaussian curves plus a constant is fit to the data in the ^{216}Po and ^{214}Po ROIs. The result for the constant (dotted horizontal line) provides an upper limit on the time-independent background in the ^{214}Po ROI $C < 0.28$ counts/day at 95% confidence.

for most of the runs in question worsened the resolution sufficiently that Gaussians provided good fits to the peaks. The upper limit on the constant value of the fit indicates $C < 0.28$ counts/day at 95% confidence in the ^{214}Po ROI.

Fig. 3 shows the average ^{214}Po background rate as a function of time. Later time bins are based on fewer runs and so have larger uncertainties. The ^{218}Po data are not used in the background analysis as there is significant overlap between the ^{210}Po and ^{218}Po peaks (see Fig. 2). This ^{214}Po data is used to estimate the background model parameters using non-linear least squares routines in the SciPy python library [8]. The model of Equation 2 is fit to the data. The parameter estimates of Equation 2 are $A = 1.06 \pm 0.36$ counts/day and $B = 1.15 \pm 0.14$ counts/day. From these estimates, the calculations of the grow-in and decay terms are $E = 1.93 \pm 0.39$ counts/day and $D_0 = 0.87 \pm 0.15$ counts/day, for $C = 0.28$ counts/day. For the best-fit value of C (0.20 ± 0.04 counts/day), $E = 2.01 \pm 0.39$ counts/day and $D_0 = 0.95 \pm 0.15$ counts/day. For $C = 0$, $E = 2.21 \pm 0.39$ counts/day and $D_0 = 1.15 \pm 0.14$ counts/day.

Also of note is the appearance of ^{212}Po and ^{216}Po peaks in the energy spectrum (Fig. 2) around 6.78 MeV and 8.79 MeV respectively. Both isotopes are radioactive progeny of ^{220}Rn. This radon isotope has a fast half-life of 55 s. It decays to ^{216}Po (half-life of 0.14 s), followed by ^{212}Pb (half-life of 10.6 hr). It is expected that ^{212}Pb is not carried with the input gas into the detection chamber. Thus, the time dependence of ^{212}Po should be from grow-in, but more data are needed to validate this prediction.

CONCLUSIONS

As expected, environmental sources of backgrounds in the alpha energy region appear to be small. A surprise is the relatively large decay term $D_0 = 0.95 \pm 0.15$ counts/day, implying that 0.044 ± 0.007 mBq of radon is transferred into the detection chamber, given the measured ^{214}Po collection efficiency of 25% [1]. This concentration is $\sim 300\times$ higher than expected from the LN boil-off gas. To attempt to reduce this background, we are now passing the input gas through a cold radon trap when performing a background run, as is regularly done for sample runs. This "cleaned"

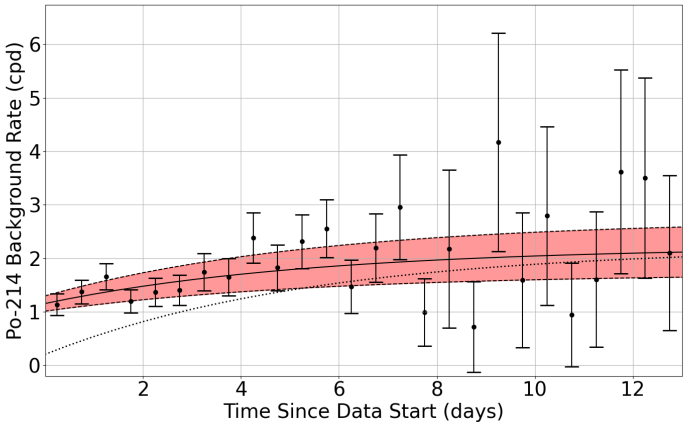

FIGURE 3. ^{214}Po background rate vs. time (filled circles with $\pm 1\sigma$ error bars) averaged over 59 background runs of varying durations, along with the best-fit of Eqn. 2 to the data (solid curve with shaded confidence interval), resulting in a $\chi^2 = 19.04$ for 24 degrees of freedom, for a p-value of 0.75. Later time bins are based on fewer runs and so have larger uncertainties. The grow-in term is significantly larger than the decay term. If the decay term were reduced to zero, *e.g.* by effective filtering of the carrier gas, the sum of the remaining grow-in plus constant terms would be the dotted curve.

background-run data will be analyzed to determine whether radon from the boil-off LN is higher than expected but can be removed. The grow-in term of $E = 2.01 \pm 0.39$ counts/day implies that 0.093 ± 0.018 mBq of radon emanates from the chamber. Work is ongoing to identify and replace the main sources of emanation in the chamber materials.

About 200 historical background runs exist. Their inclusion will allow significant improvement of the statistical uncertainties of this analysis. They will also allow a similar analysis to be performed on the ^{220}Rn chain. A time dependence can also be performed using the ^{218}Po counts, after addressing overlap from ^{210}Po. The ability of these data to help identify and mitigate the principal causes of backgrounds for the system appears promising.

ACKNOWLEDGMENTS

This work was supported in part by the Department of Energy (Grant No. DE-AC02-05CH1123). Ann Harrison performed or helped perform most of the radon emanation measurements.

REFERENCES

1. D. S. Akerib *et al.* (LUX-ZEPLIN Collaboration), "The LUX-ZEPLIN (LZ) radioactivity and cleanliness control programs," Eur. Phys. J. C **80**, 1044 (2020), arXiv:2006.02506 [physics.ins-det].
2. M. A. Bowles, *Minimizing backgrounds for the SuperCDMS SNOLAB dark-matter experiment*, Ph.D. thesis, South Dakota Mines (2019).
3. G. Audi, O. Bersillon, J. Blachot, and A. Wapstra, "The NUBASE evaluation of nuclear and decay properties," Nuclear Physics A **729**, 3–128 (2003).
4. "Laboratoire National Henri Becquerel atomic and nuclear data," `http://www.lnhb.fr/nuclear-data/nuclear-data-table/`.
5. J. Porstendorfer and T. T. Mercer, "Influence of electric charge and humidity upon the diffusion coefficient of radon decay products," Health Physics **37**, 191–199 (1979).
6. X. R. Liu, "Ultra-low level radon assays in gases," in *Proceedings of the 5th International Workshop in Low Radioactivity Techniques (LRT 2015)*, American Institute of Physics Conference Series, Vol. 1672, edited by J. L. Orrell (2015) p. 070002.
7. N. I. Chott and R. W. Schnee (for the LUX-ZEPLIN Collaboration), "Radon emanation techniques and measurements for LZ," in *Workshop on Low Radioactivity Techniques: LRT2022*, American Institute of Physics Conference Series, edited by J. Heise and R. W. Schnee (2022) these proceedings, to be published.
8. P. Virtanen, R. Gommers, T. E. Oliphant, M. Haberland, T. Reddy, D. Cournapeau, E. Burovski, P. Peterson, W. Weckesser, J. Bright, S. J. van der Walt, M. Brett, J. Wilson, K. J. Millman, N. Mayorov, A. R. J. Nelson, E. Jones, R. Kern, E. Larson, C. J. Carey, İ. Polat, Y. Feng, E. W. Moore, J. VanderPlas, D. Laxalde, J. Perktold, R. Cimrman, I. Henriksen, E. A. Quintero, C. R. Harris, A. M. Archibald, A. H. Ribeiro, F. Pedregosa, P. van Mulbregt, and SciPy 1.0 Contributors, "SciPy 1.0: Fundamental algorithms for scientific computing in Python," Nature Methods **17**, 261–272 (2020).